SCIENTIFIC REPORTS

OPEN

SUBJECT AREAS:
MOLECULAR NEUROSCIENCE
NEUROLOGICAL DISORDERS

Received
25 April 2014

Accepted
13 June 2014

Published
3 July 2014

Correspondence and requests for materials should be addressed to S.F.T.W. (Stefan.weiss@wits.ac.za)

The 37kDa/67kDa Laminin Receptor acts as a receptor for $A\beta_{42}$ internalization

Bianca Da Costa Dias[1], Katarina Jovanovic[1], Danielle Gonsalves[1], Kiashanee Moodley[1], Uwe Reusch[2], Stefan Knackmuss[2], Marc S. Weinberg[3], Melvyn Little[2] & Stefan F. T. Weiss[1]

[1]School of Molecular and Cell Biology, University of the Witwatersrand, Private Bag 3, Wits 2050, Johannesburg, Republic of South Africa, [2]Affimed Therapeutics AG, Technologiepark, Im Neuenheimer Feld 582, 69120 Heidelberg, Germany, [3]Antiviral Gene Therapy Research Unit (AGTRU), Department of Molecular Medicine & Haematology, School of Pathology, University of the Witwatersrand, Private Bag 3, Wits 2050, Johannesburg, Republic of South Africa.

Neuronal loss is a major neuropathological hallmark of Alzheimer's disease (AD). The associations between soluble Aβ oligomers and cellular components cause this neurotoxicity. The 37 kDa/67 kDa laminin receptor (LRP/LR) has recently been implicated in Aβ pathogenesis. In this study the mechanism underlying the pathological role of LRP/LR was elucidated. Försters Resonance Energy Transfer (FRET) revealed that LRP/LR and Aβ form a biologically relevant interaction. The ability of LRP/LR to form stable associations with endogenously shed Aβ was confirmed by pull down assays and Aβ-ELISAs. Antibody blockade of this association significantly lowered $A\beta_{42}$ induced apoptosis. Furthermore, antibody blockade and shRNA mediated downregulation of LRP/LR significantly hampered $A\beta_{42}$ internalization. These results suggest that LRP/LR is a receptor for $A\beta_{42}$ internalization, mediating its endocytosis and contributing to the cytotoxicity of the neuropeptide by facilitating intra-cellular $A\beta_{42}$ accumulation. These findings recommend anti-LRP/LR specific antibodies and shRNAs as potential therapeutic tools for AD treatment.

Alzheimer's Disease (AD), primarily identified by Austrian physician Alois Alzheimer in 1906[1], is a progressive neurological disorder characterised by extracellular neuritic plaques and intracellular neurofibrillary tangles (caused by aberrant misfolding and aggregation of amyloid beta peptides (Aβ) and the hyperphosphorylated tau protein), cerebrovascular amyloidosis as well as synaptic and neuronal loss. These neuropathological features are particularly evident in the basal forebrain and hippocampus, as these are the regions of higher-order cognitive function[2,3]. It is predicted that in 2050, approximately 1 in 85 people will be afflicted by the disease[4] owing to the global increase in aged populations due to enhanced life expectancies.

The transmembrane amyloid precursor protein (APP) is the parental protein from which Aβ is generated through sequential cleavage by β-secretase and γ-secretase. This cleavage may occur at the plasma membrane or within endosomes[5]. The resultant Aβ may consequently be shed into the extracellular space, be exocytosed or accumulate intracellularly.

Although extracellular neuritic plaques are a pathological hallmark of AD, the soluble intracellular oligomeric assemblies of Aβ, particularly the aggregation-prone $A\beta_{42}$ isoform, are largely considered the aetiological agents of this disease. They precede and may contribute to tau hyperphosphorylation and have been reported to directly cause synaptic and neuronal loss as well as vascular degeneration of the brain[6]. Moreover Aβ exerts its toxicity intracellularly[6] and the senile plaques themselves have been proposed to serve a neuroprotective role as Aβ sinks which sequester the toxic soluble intracellular oligomers- the peripheral sink hypothesis[7].

Although a myriad of molecular mechanisms reportedly contribute to $A\beta_{42}$ mediated neuropathology, the lack of effective therapeutics suggests that central role players in disease initiation and progression have yet to be identified. Until all the intricate pathological networks underlying AD are uncovered, effective therapeutic strategies may remain elusive. Thus, understanding the cellular trafficking as well as the associations between Aβ and cellular components (particularly cell surface receptors) are imperative to understanding its neurotoxicity.

A protein of immense interest with regards to Aβ pathogenesis is the cellular prion protein (PrP^c). PrP^c is considered neuroprotective under normal physiological conditions, through the maintenance of oxidative stress homeostasis and inhibition of β-secretase cleavage of APP[8]. In contrast, the overwhelming majority of recent

reports have demonstrated that within the AD context, PrP^c acquires a pathological role. Upon binding to Aβ oligomers (which it is able to do with high affinity, $k_D = 0.4 \times 10^{-9}M$[9,10]) PrP^c has been shown to mediate neurotoxic signals through Fyn kinase[11,12], impair synaptic plasticity, inhibit long term potentiation and contribute to intracellular accumulation of Aβ by mediating the internalization of Aβ oligomers[13]. However, owing to the glycosylphosphatidylinositol (GPI)-anchored nature of this protein[14], it is largely dependent on its receptors to mediate the aforementioned functions. One such receptor, which exhibits a high binding affinity ($k_D = 1 \times 10^{-7}$ M) for PrP^c, is the 37 kDa/67 kDa laminin receptor (LRP/LR) (also known as LamR, RPSA and p40)[15]. This multifunctional receptor is implicated in numerous physiological roles including translation, maintenance of cytoskeletal structure[16], cell survival, differentiation, proliferation and migration[17,18]. LRP/LR is also involved in the development of numerous pathological states, including cancer[18,19] and tumour angiogenesis[20], prion disorders and both viral[21–24] and bacterial infections (of particular interest being bacterial meningitis as the receptor mediates translocation across the blood brain barrier)[25].

As LRP/LR serves as a PrP^c receptor we aimed to investigate whether LRP/LR is implicated in Aβ pathogenesis. Antibody blockade and shRNA mediated downregulation of LRP/LR was shown to significantly enhance the viability and proliferative potential of cells treated with $A\beta_{42}$[26]. In this study we aimed to further probe the mechanism underlying the role of LRP/LR in mediating Aβ pathogenesis.

Results

Försters resonance energy transfer between cell surface LRP/LR and Aβ. Försters resonance energy transfer (FRET) is one of the most sensitive techniques employed to assess protein interactions in cellular systems. The non-radiative energy transfer from a donor to an acceptor will only occur if the fluorochromes are within 1–10 nm from each other. A cytometry-based FRET assay was employed to investigate whether LRP/LR and Aβ interact on the surface of HEK293 cells. The highly sensitive[27,28] PE/APC FRET pair (donor and acceptor, respectively) was employed to immunolabel the proteins of interest on non-permeabilised cells. As PE is maximally excited by the 488 nm argon laser and emits maximally at 575 nm it may be detected with the FL2 filter set of the Accuri C6 (BD Biosciences),whilst APC, excited by the 650 neon/helium laser and exhibiting maximal emission at 660 nm, is readily detectable with the FL4 filter set (Fig. S1). Successful labelling of the proteins of interest (LRP/LR, PrP^c, CAT and Aβ) was confirmed (Fig. S2). The presence of FRET between the proteins of interest was evaluated employing the FL3 filter set. Within this channel, excitation is achieved with the 488 nm argon laser and emission of 660 nm is detected. The APC antibody is not excited and does not exhibit fluorescence within this channel. This therefore accounts for the overlay between unlabelled cells; cells labelled solely with the APC secondary antibody as well as cells in which PrP^c, CAT and Aβ were immunolabelled with APC (Fig. 1a,c,e). However, upon the close proximity of the PE-coupled secondary antibody, APC may be indirectly excited via FRET, and this may result in the enhanced fluorescence emission of the acceptor in FL3 (Fig. S1). It is owing to this that FL3 is considered the optimal channel for FRET detection between the PE/APC pair.

The efficacy of this flow cytometry based FRET assay was investigated employing PrP^c, a cell surface protein to which LRP/LR binds with very affinity[15] (positive control) and chloramphenicol acetyl transferase (CAT), a bacterial protein to which LRP/LR has been shown to not bind[26] (negative control). Upon co-labelling of cells with PrP^c-APC with LRP/LR-PE, the fluorescence of APC was enhanced, as was observed by the rightward shift of the APC histogram along the FL3 fluorescence intensity axis (Fig. 1b). Conversely co-labelling of CAT-APC with LRP/LR-PE had no effect on the emission of APC, as was evident by the overlay between the two histograms (Fig. 1d). The augmentation of APC fluorescence intensity upon co-labelling of cells with Aβ-APC and LRP/LR-PE (Fig. 1f), therefore suggests that FRET occurred between these proteins.

LRP/LR interacts with shed Aβ. To confirm that LRP and Aβ form stable associations, pull down assays were conducted. Although similar experimental procedures have been previously reported[26], these were conducted employing exogenously administered synthetic $A\beta_{42}$ peptide. Those reported here employed conditioned cell culture media (supernatant) from HEK293 cells into which Aβ was shed, thereby investigating the presence of this association within a physiological context. The averaged total concentration of Aβ present in the conditioned media was approximately 37.6 pg/ml, results which are consistent with the concentration of Aβ detected by others in the supernatant of HEK293 cells[29]. The efficacy of this assay was confirmed by the presence of both the BAP-fusion protein (~49 kDa) and LRP::FLAG (~38 kDa) in the eluted samples, which indicates that these proteins were successfully immobilized by the Anti-FLAG® M2 beads (~17 kDa) (Fig. 2a, lane 4). The presence of CAT (~26 kDa) in the unbound sample (Fig. 2a, lane 1), reveals that this protein was not immobilised by LRP::FLAG and further confirms that CAT does not interact with LRP. Evaluation of the degree of Aβ present in each pull down assay fraction required sensitive detection employing an Aβ- specific ELISA assay. Upon co-incubation of conditioned media with LRP::FLAG containing cell lysate, it was observed that Aβ was successfully immobilized by LRP:FLAG, as there was a significant increase (27%) ($p = 0.0433$) in the Aβ levels in the eluate sample when compared to that present in wash 3 (Fig. 2b). To account for possible binding of Aβ to other proteins within the cell lysate or non-specific binding to the Anti-FLAG® M2 beads, the degree of Aβ in the eluates of samples containing conditioned media co-incubated with NT lysates or conditioned media alone, were compared to LRP::FLAG containing samples (Fig. 2c). There was a significant increase in the amount of Aβ bound to the column in the presence of LRP::FLAG when compared to that in NT lysates (34%) ($p = 0.039611287$) and conditioned media alone (19%) ($p = 0.04788224$). It is noteworthy to add that the degree of Aβ present in the eluate was not significantly different to that in wash 3 in both NT lysate (Fig. S3a) and conditioned media only samples (Fig. S3b). It must be noted that the ELISA employed to quantify the concentration of Aβ is unable to distinguish between the $A\beta_{40}$ and $A\beta_{42}$ isoforms.

Cellular incubation with $A\beta_{42}$ induces apoptosis. An Annexin-V-7AAD assay was employed to assess the cellular effects of synthetic $A\beta_{42}$ on HEK293 cells. The exogenous application of 200 nM and 500 nM $A\beta_{42}$ did not produce cytotoxic effects after 24 h (Fig. 3a) but did result in a progressive induction of apoptosis after 48 h. Apoptosis induction was concentration dependent with the degree of apoptosis detected after 72 h being approximately 30% greater in the 500 nM treatment when compared to the 200 nM treatment (Fig. 3a).8 mM PCA, an apoptosis inducing agent, was employed as a positive control and was similarly assessed over 72 h. The time-dependent induction of apoptosis was confirmed by the nuclear morphological changes observed in cells treated with 500 nM $A\beta_{42}$ (Fig. 3b). At 24 h, most nuclei appeared normally stained but 48 h post-treatment, the first stage of chromatin condensation, namely chromatin condensation around the nuclear periphery, was observed. Post 72 h treatment, apoptotic bodies were detectable (Fig. 3b).

IgG1-iS18 rescues cells from Aβ induced apoptosis. The degree of cell death (comprising early and late apoptosis as well as necrosis) induced upon cellular treatment with 200 nM and 500 nM

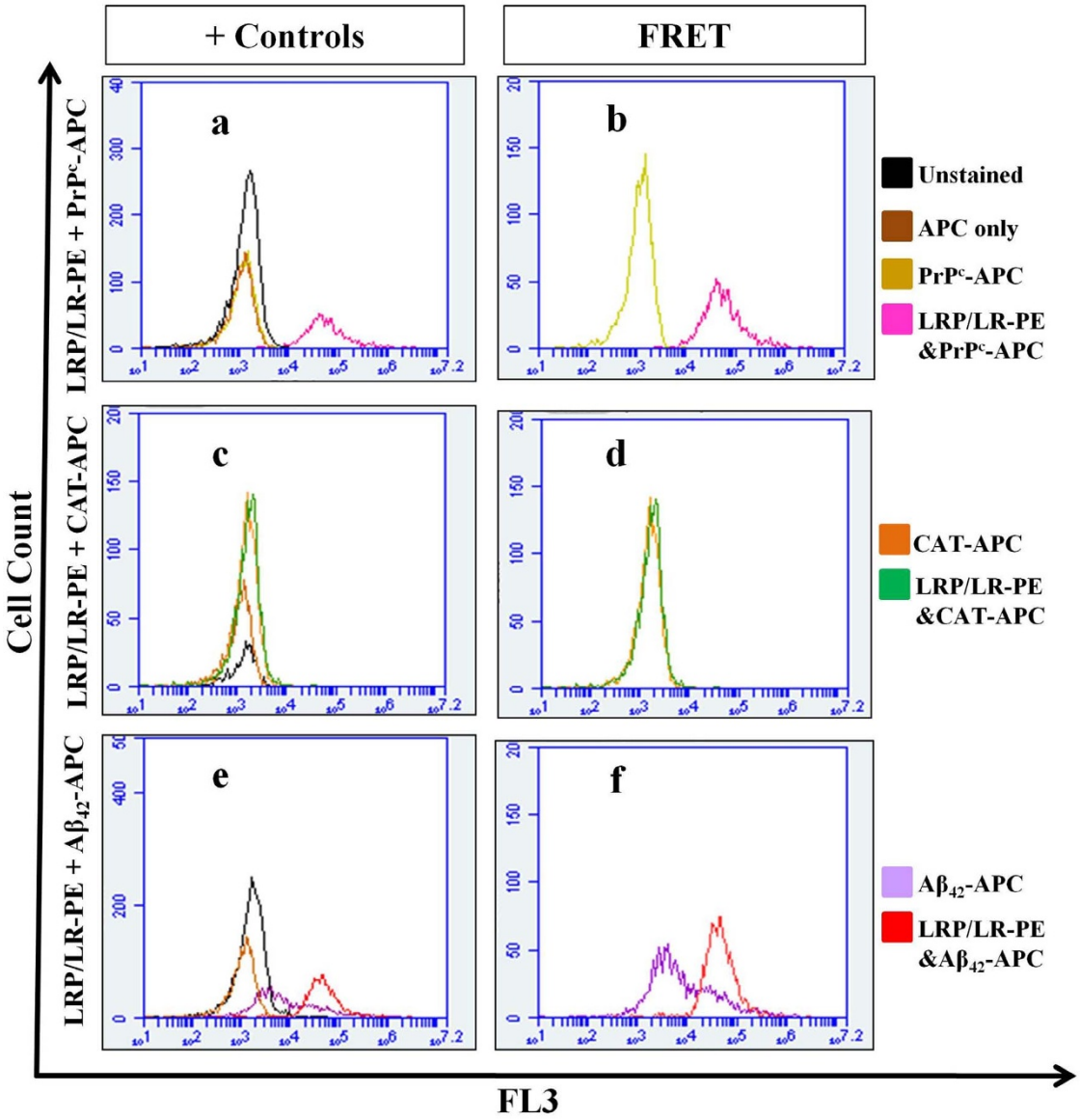

Figure 1 | Flow cytometric analysis of Försters Resonance Energy Transfer (FRET) between cell surface LRP/LR and Aβ. The fluorescence intensity histogram of the unlabelled non-permeabilised HEK293 cells (black histogram, a,c,e) was superimposed with that of cells labelled with the APC secondary antibody only (brown histogram, a,c,e) as well as with cells in which the proteins of interest (PrP^c, CAT and $A\beta_{42}$) were labelled with APC (a,c,e respectively). Co-labelling of LRP/LR-PE and PrP^c-APC (positive control) (pink histogram, b). Co-labelling of LRP/LR-PE and CAT-APC (negative control) (green histogram, d). Co-labelling of LRP/LR-PE and Aβ-APC (red histogram, f). Each panel is a representative image. Three biological replicates, each performed in triplicate, were conducted.

exogenous synthetic $A\beta_{42}$ for 72 h was assessed by Annexin-V-7AAD assay. Upon assessment, cellular incubation with 200 nM $A\beta_{42}$ resulted in 53.6% cell death, whilst treatment with 500 nM $A\beta_{42}$ resulted in 78.84% cell death (Fig. 4). In both treatments, apoptosis accounted for >85% of the detectable cell death. Co-incubation of the cells with 50 μg/ml IgG1-iS18 (anti-LRP/LR specific antibody) significantly reduced the extent of cell death induced by $A\beta_{42}$ at both concentrations by 45.35% ($p < 0.001$) and 57.39% ($p < 0.001$), respectively whilst the anti-CAT antibody (negative control) had no effect on cell death processes (Fig. 4). Protocatechuic acid (PCA), an apoptosis inducing agent, was employed as the positive control. Antibody treatment with IgG1-iS18 alone does not significantly reduce cell death when compared to the untreated control (Fig. 4).

$A\beta_{42}$ internalization. The degree of cell surface $A\beta_{42}$ served as a measure of the degree of receptor-mediated internalization - with lower cell surface $A\beta_{42}$ levels being indicative of enhanced internalization, whilst higher levels reveal reduced internalization or recycling. Cellular incubation of control cells at 4°C prior to and after exogenous $A\beta_{42}$ administration was performed to limit internalization as receptor-mediated internalization is halted under these conditions. Thus, the cell surface levels of $A\beta_{42}$ in the no internalization control (1 h, 4°C) was set to 100%. The progressive decrease in cell surface $A\beta_{42}$ may therefore be interpreted as a consequence of receptor-mediated internalization of the exogenous $A\beta_{42}$. Although internalization (12.05%) was observed after 5 min, the extent of $A\beta_{42}$ internalization was at its highest and most evident after 15 min (66.9%) after which the level of cell surface $A\beta_{42}$ remained relatively constant for a further 15 min and then increased (Fig. 5a). The significant 11.36% increase ($p < 0.001$) in cell surface $A\beta_{42}$ at 1 h when compared to 30 min may be indicative of $A\beta_{42}$ recycling to the cell surface (and ultimately exocytosis) by the cell. The internalization of the exogenously administered $A\beta_{42}$ was

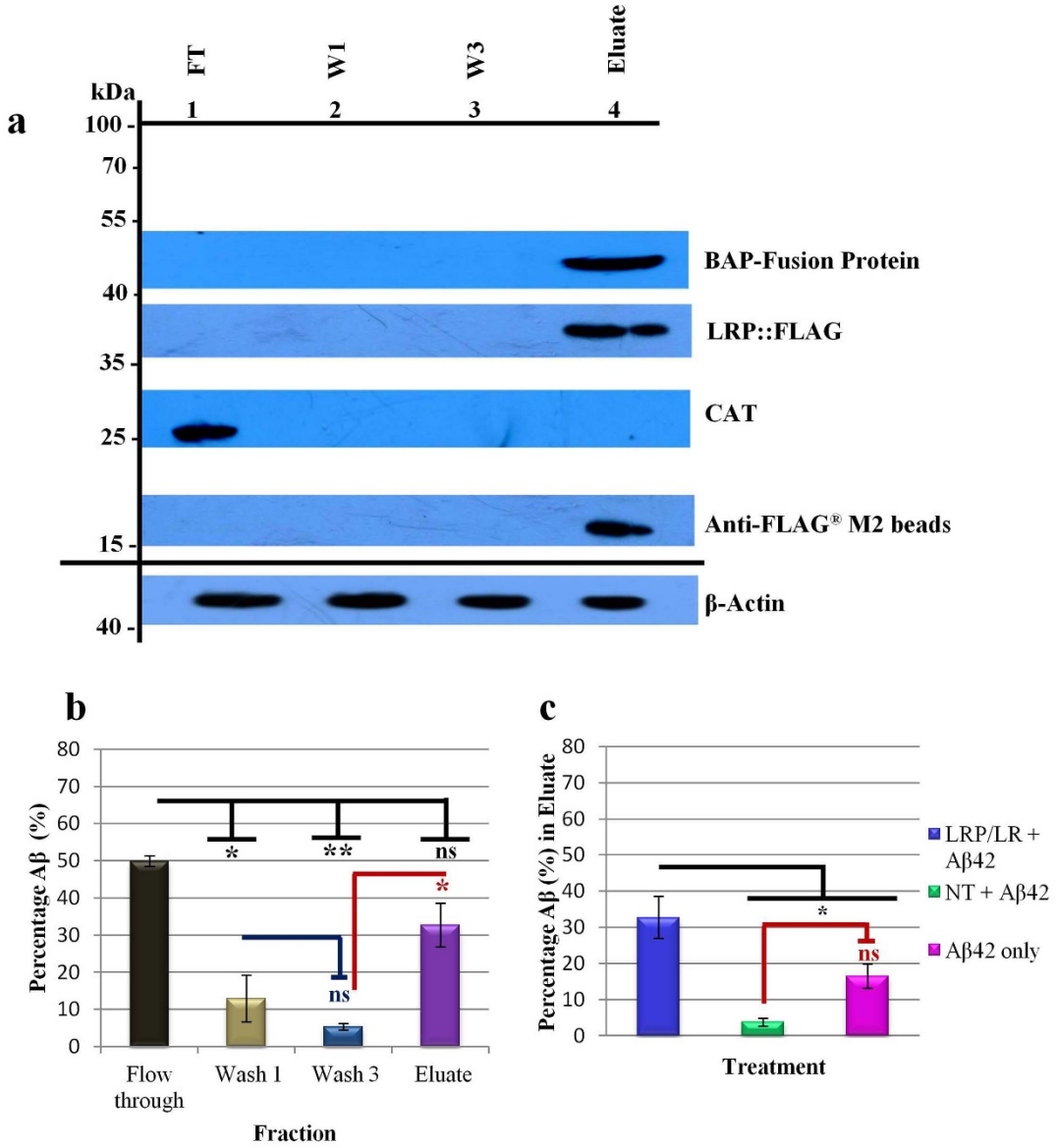

Figure 2 | FLAG® Immunoprecipitation Assays demonstrate LRP/LR-Aβ association. HEK293 cell lysates, non transfected as well as lysates containing recombinant LRP::FLAG to which either recombinant CAT lysates (negative control), BAP-Fusion protein (positive control) or conditioned tissue culture media containing Aβ was added, were subjected to pull down assays. Samples were analysed by Immunoblotting (a) Lane 1, unbound sample (flow through); lane 2, first wash step (W1); lane 3, third wash step (W3) and lane 4, eluate samples. β-actin served as the loading control. Fraction sample of pull down assays containing conditioned media were assessed by Aβ-ELISA (b & c). The Aβ levels per fractions of the LRP::FLAG pull down were detected by Aβ ELSA (b).The Aβ levels present in eluate of: LRP::FLAG lysate & conditioned media sample; NT lysate & conditioned media and conditioned media alone are depicted (c). Gels have been cropped for clarity and conciseness purposes and we all run under the same experimental conditions. Data shown are representative (mean ± s.e.m.) of three biological replicates, each performed in triplicate. *$p < 0.05$, **$p < 0.01$; Student's *t*-test.

further confirmed by confocal microscopy. Cells were previously transfected with pCFP-mem such that the plasma membrane could be readily identified. At 5 min, it is evident that most of the $A\beta_{42}$ is located at the cell surface whilst at 15 min and more markedly at 30 min, the degree of $A\beta_{42}$ labelling within the cell lumen is unmistakably enhanced. As 100 nM $A\beta_{42}$ is considered to be below the detection limit for intracellular immunostaining[6], microscopic visualization was only attained upon cellular treatment with 500 nM, to ensure dependable results were obtained. It is noteworthy to add that very high cell densities negatively affect ligand binding efficiencies and thus 70% densities were considered optimal for successful internalization. Furthermore, cell signalling and receptor-mediated internalization events were synchronized as a result of serum starvation prior to experimentation[30].

LRP/LR is a central mediator of $A\beta_{42}$ internalization. The degree of cell surface $A\beta_{42}$ served as a measure of the degree of receptor-mediated internalization. Cells were either subjected to antibody treatment (Fig. 6a) or RNA intereference technology in which LRP/LR was downregulated by shRNA7.6 (Fig. 6b)[29]. All relevant controls were similarly incubated at 4°C, prior and post exogenously 500 nM $A\beta_{42}$ administration as this halts receptor-mediated internalization processes[30]. The cell surface levels of $A\beta_{42}$ in the untreated no internalization control (1 h, 4°C) was set to 100% in both experimental sets (Fig. 6a & 6b). Upon, co-incubation of cells with 50 μg/ml IgG1-iS18 (anti-LRP/LR specific antibody), a significant enhancement in cell surface $A\beta_{42}$ was observed across all incubation periods when compared to untreated controls at corresponding time points (Fig. 6a). This therefore demonstrates

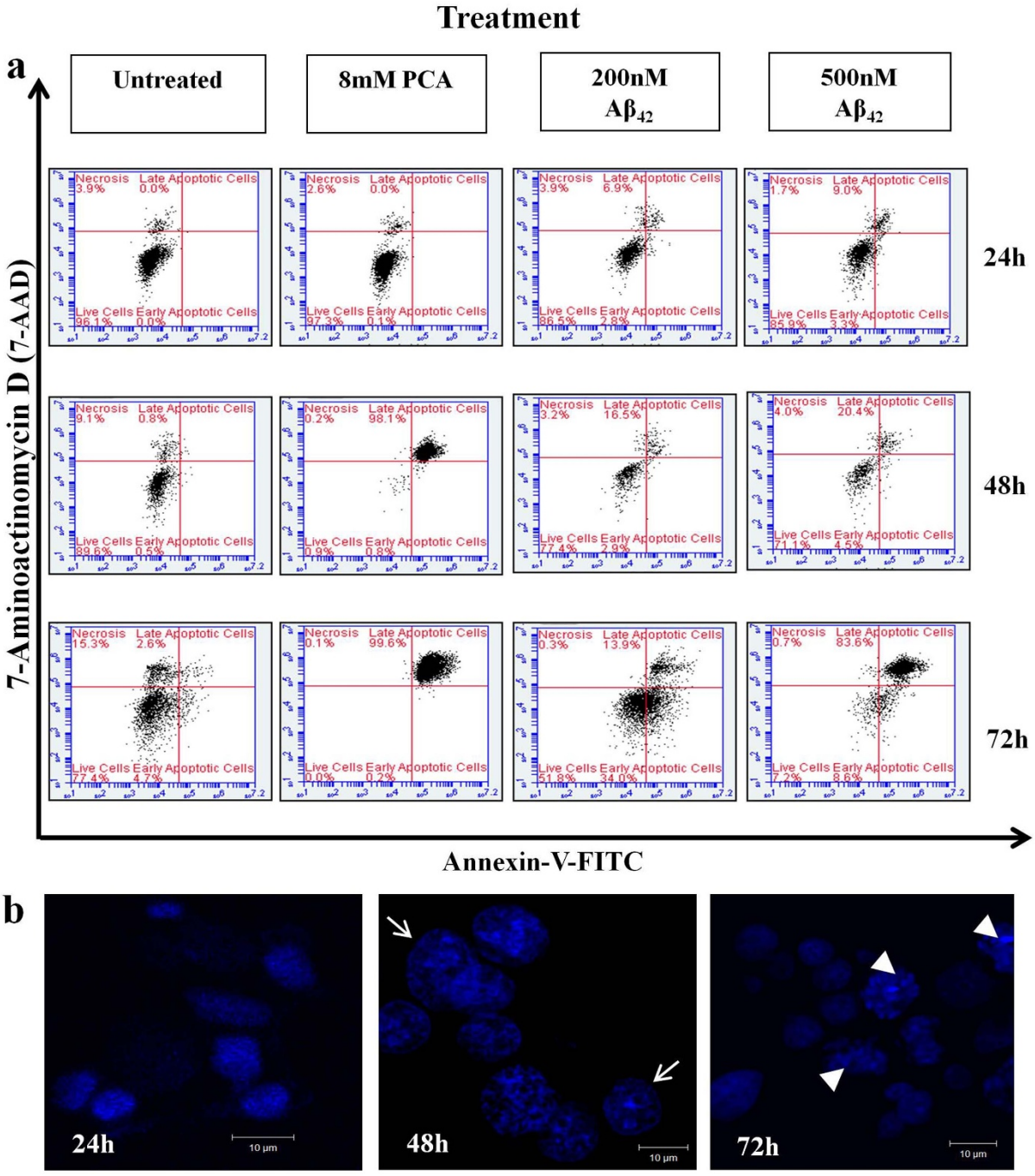

Figure 3 | $A\beta_{42}$ treatment induces apoptosis. The induction of cell death in HEK293 cells treated with 200 nM or 500 nM $A\beta_{42}$ for different incubation periods, was assessed by Annexin-V-7AAD assay (a). The induction of apoptosis was further confirmed by assessing the nuclear morphology at 24 h, 48 h and 72 h post-treatment with 500 nM $A\beta_{42}$ (b). Arrows depict chromatin condensation against the nuclear periphery, arrow heads depict apoptotic bodies. Figures shown are representative images. Three biological replicates, each performed in triplicate, were conducted per experiment.

that antibody blockade of LRP/LR resulted in more cell surface-associated $A\beta_{42}$ across all time points (in comparison to untreated controls) and this therefore suggests that $A\beta_{42}$ internalization is hampered as a result of LRP/LR antibody blockade. Cells similarly treated with the anti-CAT antibody displayed $A\beta_{42}$ internalization processes analogous to those of untreated controls (Fig. 6a). Furthermore, antibody treatment alone, in the absence of $A\beta_{42}$, did not significantly alter internalization processes.

To confirm that LRP/LR is indeed implicated in $A\beta_{42}$ internalization, and the effects observed during IgG1-iS18 treatment were not owing to steric effects of the antibody on surrounding proteins, LRP/LR was downregulated employing short hairpin RNAs (shRNAs). When compared to the shRNA scrambled (shRNA scr) controls (at corresponding incubation points), LRP/LR downregulation as mediated by shRNA7.6, significantly enhanced the degree of cell surface $A\beta_{42}$ and therefore impeded internalization (Fig. 6b). The transfection methodology itself did not adversely affect the internalization processes, as the difference in cell surface $A\beta_{42}$ levels was not significantly different between control, mock transfected and shRNAscr samples across all incubation periods (Fig. 6b).

Flow cyometric analysis confirmed that shRNA7.6 resulted in a significant 55.4% decrease ($p = 0.008$) in cell surface LRP/LR levels when compared to the shRNA scr (Fig. 6c). This was evidenced as a shift towards a lower fluorescence intensity when the fluorescence

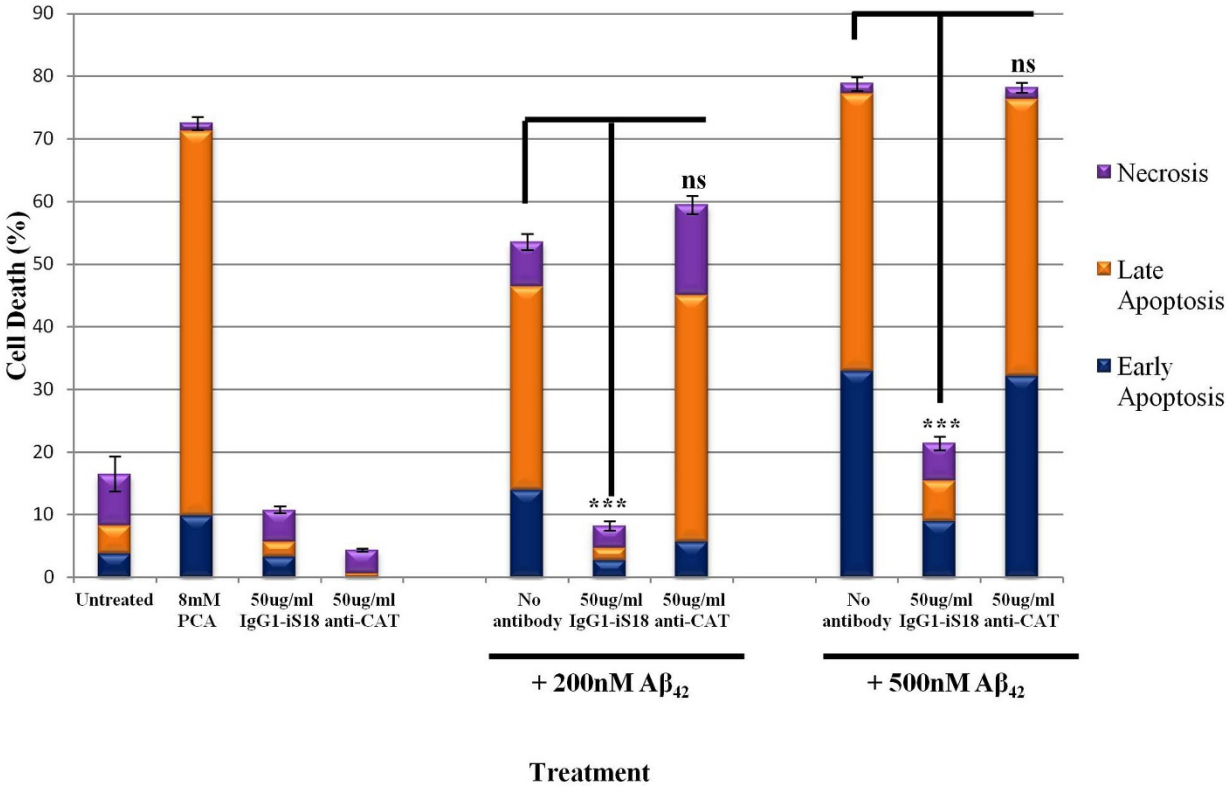

Figure 4 | Cell rescuing effects of anti-LRP/LR antibody IgG1-iS18. Cell death of HEK293 cells, assessed by Annexin-V-7AAD assay, post exogenous treatment with 200 nM and 500 nM synthetic $A\beta_{42}$ and upon co-incubation with anti-LRP/LR IgG1-iS18 or anti-CAT (negative control). Cell death was assessed 72 h post treatment. No antibody control was set to 100%. Data shown are representative (mean ± s.d.) of three biological replicates, each performed in triplicate. *$p < 0.05$, **$p < 0.01$, ***$P < 0.001$; Student's *t*-test.

intensity histograms of both treatments are overlayed (Fig. S4a). The LRP/LR fluorescence intensity histograms of control, mock and shRNA scr controls overlayed perfectly (Fig. S4b) and the median fluorescence intensities (MFI) of these treatments were not significantly different to that of the untreated control (set to 100%) (Fig. S4c). These results confirm that the transfection methodology did not alter cell surface LRP/LR expression levels. To assess whether LRP/LR downregulation may influence cell surface PrP^c levels, which would confound the observed results, the cell surface expression of PrP^c was evaluated. Flow cytometric analysis of shRNA transfected cells revealed that LRP/LR downregulation had no significant effect on cell surface PrP^c levels (Fig. 6d). Similarly the PrP^c fluorescence intensity histograms of control, mock and shRNA scr controls overlayed perfectly (Fig. S4d) and the MFIs of these treatments were again not significantly different (Fig. S4e). Thus, PrP^c cell surface expression levels were not affected by the transfection methodology.

Discussion

Ensuring that LRP/LR and $A\beta_{42}$ interact naturally preceded investigations regarding the mechanism underlying the receptor's role in AD pathogenesis. We have previously demonstrated that LRP/LR and Aβ co-localize on the surface of HEK293 and N2a cells[26], results which suggested that a potential interaction may exist between these endogenously expressed proteins. However, co-localization has a resolution limit of 200 nm and therefore positive results may not necessarily be indicative of an association, but may simply demonstrate that proteins share similar cellular locations. This would be expected as Aβ has been reported to insert into the lipid raft region of the plasma membrane, the region to which LRP/LR is localized[31]. Therefore, in order to probe the potential of such an interaction existing under normal cellular conditions, Försters resonance energy transfer (FRET) was employed. FRET is based on the principle that a donor fluorochrome (phycoerythrin (PE) in this study), within 1–10 nm of the acceptor fluorochrome (allophycocyanin (APC)), will non-radiatively transfer energy to the acceptor and this, depending on the FRET couple chosen, may result either in the enhanced fluorescence emission of the acceptor[32] or acceptor bleaching. The former is detected upon using the PE/APC FRET couple employed in this study. The PE/APC FRET pair was selected as the fluorochromes exhibit very high molar extinction coefficients (1 200 000 $M^{-1}cm^{-1}$ and 5000 $M^{-1}cm^{-1}$, respectively) and quantum yields and this makes them exceptionally sensitive when coupled to antibodies[28] and may achieve 90% FRET efficiencies[28]. Furthermore, although microscopy is classically employed to assess FRET, the tedious nature and inability to analyse large cell numbers, led researchers to apply flow cytometric detection methods instead. The efficacy and accuracy of this technique was assessed by investigating whether FRET was observed between LRP/LR and known ligands to which it either binds with high affinity (PrP^c) or has been shown not to bind (CAT). APC, a fluorochrome not excited by the 488 nm laser, either alone or employed to label a protein of interest, did not exhibit fluorescence emission in the FL3 channel (which employs 488 nm for excitation and a 660 filter set for emission detection) as the fluorescence intensity was superimposed on that obtained from unlabelled cells (Fig. 1a,c,e). This therefore demonstrates that the fluorescence detected within the FL3 channel for unstained, APC only as well as APC labelling of proteins of interest (PrP^c, CAT and $A\beta_{42}$) was owing to the native fluorescence of the cells. However, upon co-labelling of PrP^c -APC and LRP/LR-PE, the fluorescence intensity of APC was notably augmented (Fig. 1b) whilst co-labelling of CAT-APC and LRP/LR had no such effect (Fig. 1d). This therefore correctly implies that LRP/LR and PrP^c interact and this in turn allowed FRET to transpire. Since CAT and LRP/LR do not interact[26], the absence of FRET was expected. The occurrence of FRET between LRP/LR and

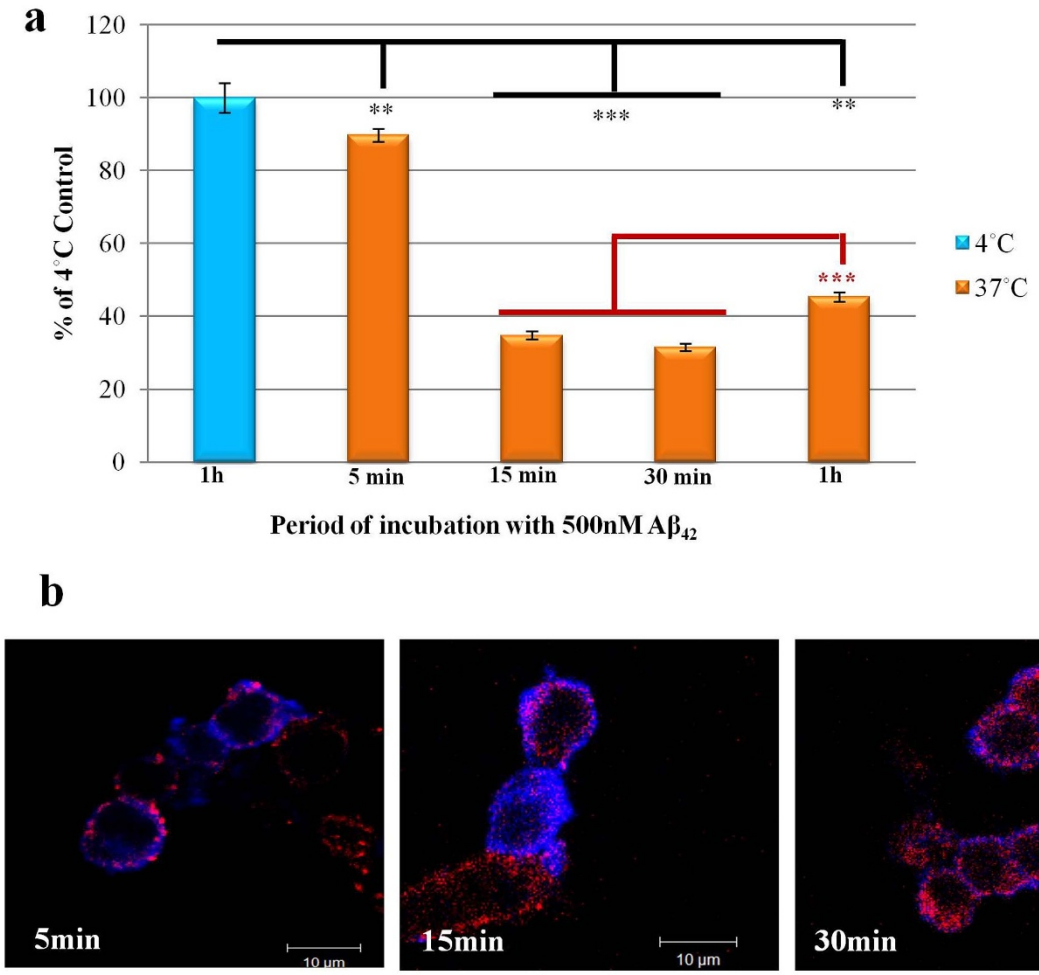

Figure 5 | $A\beta_{42}$ Internalization. The degree of cell surface Aβ served as a measure of the degree of receptor-mediated internalization. The cell surface levels of Aβ in the no internalization control (1 h, 4°C) was set to 100% (a). $A\beta_{42}$ internalization was confirmed by assessing the degree of intracellular $A\beta_{42}$ in HEK293 cells. Cells were transfected with pCFP-mem, resulting in plasma membrane labelling (depicted in blue). Intracellular Aβ was labelled with Anti-β-amyloid-APC (depicted in red) (b). Data shown are representative (mean ± s.d.) of three biological replicates, each performed in triplicate. *$p < 0.05$, **$p < 0.001$; Student's *t*-test.

Aβ (Fig. 1f) therefore suggests that these proteins are within 10 nm if each other on the cell surface and the most probable consequence thereof is that these proteins interact. Flow cytometric analysis of FRET, employing the PE/APC fluorochrome couple, has been successfully employed to identify other biologically relevant molecular interactions[28,33].

To confirm that a stable physiological association does indeed exist between LRP/LR and Aβ pull down assays were performed. Although a similar experiment has been previously performed[26], high quantities (2 μg) of synthetic $A\beta_{42}$ were utilized and thus the presence of this interaction under normal physiological conditions warranted investigation. A significantly higher proportional of shed Aβ was present in the eluate of samples containing recombinantly expressed LRP:FLAG when compared to samples containing NT cell lysate and conditioned media alone (Fig. 2c) thereby suggesting that endogenously expressed and shed Aβ was successfully immobilized by LRP/LR and that a physiologically relevant association exists between these proteins. In addition, inadequate washing and disruption of non-specific associations between Aβ and the LRP:FLAG containing column can be discounted as contributors to the high levels of immobilized Aβ as the proportion of Aβ present in the wash step 3 fraction was significantly lower than that in the eluate (Fig. 2b). Moreover, the degree of immobilized Aβ in the eluates of the control samples were not significantly different from the proportion present in the wash step 3 fraction (Fig.S3a & S3b) nor significantly different from each other (Fig. 2c), and can therefore be attributable to a low degree of non-specific binding of Aβ to the column as the results suggest that no proteins present in the NT lysate were able to mediate Aβ-column binding.

The interaction of Aβ with cell surface receptors has been repeatedly shown to lead to pathological events, including aberrant cell signalling pathways and the induction of cell death. Although apoptosis is the more common cell death modality observed, necrosis has also been suggested to underlie Aβ neurotoxicity[34] owing to the deregulation of intracellular Ca^{2+} levels which are a consequence of Aβ insertions into the plasma membrane[35] and adverse effects on cellular endoplasmic reticula and mitochondria. Therefore, the form of cell death induced upon Aβ treatment was assessed by Annexin-V-7AAD assay and the induction of apoptosis (which accounted for >85% of the cell death) was demonstrated to be both time and concentration dependent (Fig. 3a). Antibody blockade of LRP/LR, as achieved by co-incubation of the cells with IgG1-iS18 (anti-LRP/LR specific antibody) and 500 nM $A\beta_{42}$, significantly lowered the degree of apoptosis induced by the neurotoxic peptide in comparison to untreated and isotype antibody (anti-CAT) treated controls (Fig. 4). From these results it may be proposed that upon binding to Aβ, LRP/LR may stimulate/promote pro-apoptotic processes.

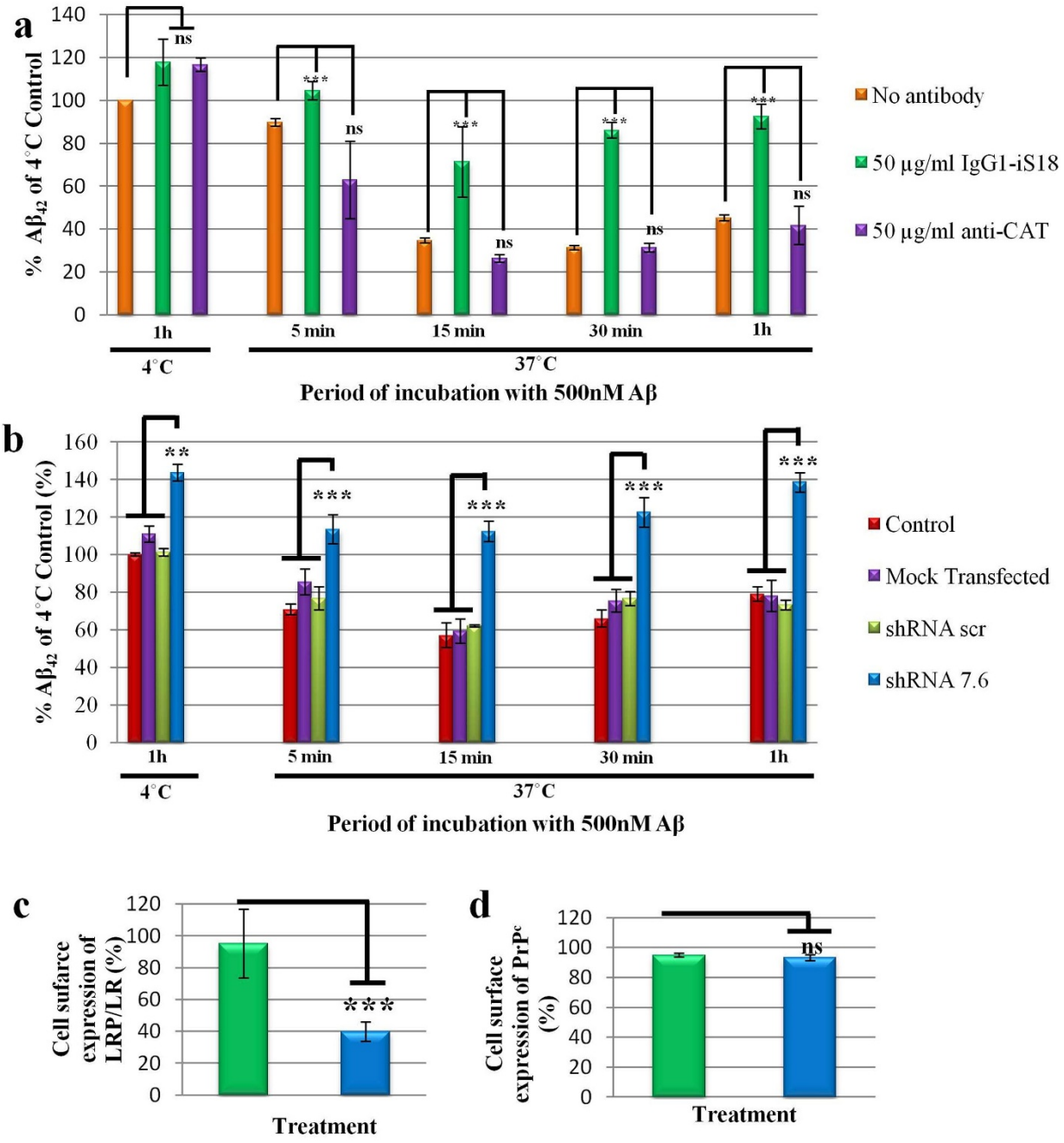

Figure 6 | Effects of antibody blockage and shRNA downregulation of LRP/LR on $A\beta_{42}$ internalization. HEK293 cells were subjected to antibody treatment: 50 µg/ml IgG1-iS18 (anti-LRP/LR specific antibody) or anti-CAT(negative control) (a) or transfected with shRNA 7.6 (against LRP/LR) (b). The degree of cell surface Aβ served as a measure of the degree of receptor-mediated internalization. The cell surface levels of Aβ in the no internalization control (1 h, 4°C) was set to 100% in both data sets. Successful downregulation of cell surface LRP/LR levels post shRNA downregulation was confirmed by flow cytometry (c). Cell surface PrP^c levels were unaffected by shRNA mediated downregulation of LRP/LR (d). Data shown are representative (mean ± s.e.m.) of three biological replicates, each performed in triplicate. *$p < 0.05$, **$p < 0.01$, ***$p < 0.001$; One way ANOVA.

This may be achieved through aberrant cell signalling. The cellular survival and proliferative role's of LRP/LR are reportedly realized through the Mitogen activated protein (MAP) kinase signal transduction pathway[36]. LRP/LR has been suggested to transduce cell survival and proliferative signals through the MAPK signalling pathway[36] upon binding to laminin-1[37]. LRP/LR regulates the expression of MAPK phosphatases (MKP1 and PAC1) and may thereby influence the activities of JNK, ERK1/2 and p38[36]. Marked MAPK deregulation ensues in AD[38]. The possibility that Aβ binding to LRP/LR may foil the receptor binding to physiologically relevant ligands such as laminin-1 and thereby perturb its normal physiological functions- which may contribute to deregulation, cannot be excluded. This would not be an unique occurrence, as epigallocatechin 3-*O*- gallate (EGCG) mediates its apoptotic activity through binding to LRP/LR[39]. Thus, despite its role in maintaining cell survival under physiological conditions, LRP/LR may gain pathological functions upon binding to certain ligands.

In addition, a multitude of research has demonstrated that Aβ binding to PrP^c leads to the induction of apoptosis through an upregulation of pro-apoptotic proteins such as Bax[40], enhanced Ca^{2+} release into the cytosol[41] and the activation of caspases- particularly caspase 8[41]. However, these pro-apoptotic signals may not be directly

transduced by PrP^c as it is not a transmembrane protein and therefore must be transduced through receptors to which PrP^c binds. We have recently demonstrated that LRP/LR does indeed contribute to PrP^c-$A\beta_{42}$ mediated cell death [Unpublished data, Pinto, M.G., Jovanovic, K., Da Costa Dias, B., Knackmuss, S., Reusch, U., Little, M. & Weiss, S.F.T. The 37kDa/67kDa LRP/LR plays a central role in Aβ-PrP^c mediated cytotoxicity in Alzheimer's disease, (2014).].

Therefore, these data suggest that LRP/LR may, either directly or indirectly, mediate $A\beta_{42}$ induced apoptosis.

It is important to note that this finding is physiologically relevant as the $A\beta_{42}$ concentrations within AD brains have been reported to be within the 200–4500 nM $A\beta_{42}$ range[42].

Furthermore, it must be noted that at nM concentrations, such as those employed in this study, $A\beta_{42}$ exists largely as low molecular weight oligomers[43]. Moreover, it has been demonstrated that even upon incubation in cell culture media, low nM concentrations of synthetic $A\beta_{42}$ (0–500 nM) do not aggregate to form higher order, less toxic fibrils[44]. Based on these findings, it may be safely proposed that the biological effects observed herein may largely be attributable to oligomeric $A\beta_{42}$, the neurotoxic species in AD.

However, as previously noted, the toxicity of Aβ is largely considered to be caused by its intracellular accumulation and aggregation- the levels of intracellular soluble Aβ are approximately 70 fold greater in AD brains compared to healthy age-matched controls[45]. Moreover it may be the ability of Aβ to incite misfolding and aggregation amongst cellular proteins which consequently leads to the deregulation of cellular processes. Therefore, it was imperative to examine whether the exogenously administered $A\beta_{42}$ was internalized into the cells. Internalization was evident from the earliest time point (5 min) and most pronounced after 15 min. However, evidence for Aβ intracellular trafficking and recycling to the cell surface (possibly along its exocytosis pathway) was apparent as the cell surface Aβ levels increased after 1 h (Fig. 5a).

LRP/LR was shown to be a central receptor in mediating the internalization of $A\beta_{42}$ as antibody blockade of the receptor significantly augmented cell surface-associated $A\beta_{42}$ and this thereby demonstrated that the amount of $A\beta_{42}$ internalized was lessened, especially at the time points 15 min, 30 min and 1 h (Fig. 6a). These results were further corroborated by shRNA mediated downregulation of LRP/LR (Fig. 6b) and thereby demonstrated that the effects observed were not due to a lack of antibody specificity. The increase in cell surface Aβ levels observed at 4°C in cells in which LRP/LR was downregulated compared to control samples (Fig.6b) may be attributable to reduced rates of PrP^c internalization, thereby allowing for enhanced Aβ binding.

This may be readily justified by the fact that PrP^c, a ligand to which LRP/LR binds with high affinity, has been firmly established as a protein required for Aβ internalization[13]. However as PrP^c lacks a transmembrane domain, its ability to mediate this internalization is dependent on its association with transmembrane receptors. LRP/LR serves a vital role in mediating PrP^c internalization into endosomes and cellular trafficking, results which have been confirmed in various neuronal cell types[46,47]. LRP/LR accounts for 25–50% of PrP^c internalization[15]. The fact that blockade of the receptor did not completely abrogate $A\beta_{42}$ internalization (Fig. 6a) may be due to the fact that only approximately 50% of $A\beta_{42}$ bound to the neuronal surface is internalized via PrP^c-dependent mechanisms[48]. It is noteworthy to add that heparan sulphate proteoglycans (HSPGs), to which LRP/LR similarly binds, have also been reported to mediate Aβ internalization[6].

Furthermore LRP/LR is not the sole PrP^c-binding protein implicated in its internalization, other such receptors include N-methyl-D-aspartate (NMDA) receptors[49], metabotropic glutamate receptor 5 (mGluR5)[50] and low-density lipoprotein receptor related protein (LRP1)[13], and these may therefore account for the internalization of $A\beta_{42}$ evident during antibody treatment.

It was due to this essential role of PrP^c, that possible downregulation of PrP^c as a consequence of LRP/LR downregulation needed to be negated (Fig. 6d). As cell surface PrP^c remained unaltered in cells exhibiting reduced LRP/LR (Fig. 6c and 6d), results which are comparable to those observed when RNAi methodologies were employed to downregulate LRP/LR *in vitro*[51], the central role of LRP/LR in Aβ internalization was validated.

Further studies are currently underway to examine whether LRP/LR mediates the internalization of Aβ directly, in the absence of PrP^c, or whether LRP/LR serves as the scaffold protein required for the internalization of the PrP^c-$A\beta_{42}$ complex.

In conclusion, it has been demonstrated that LRP/LR serves as a biologically relevant receptor of Aβ. This ubiquitously expressed receptor occupies a central role in mediating $A\beta_{42}$ internalization and may thereby contribute to the intracellular accumulation of the neurotoxic peptide and the consequent induction of apoptosis. Furthermore, specific antibodies and shRNAs directed against the 37 kDa/67 kDa laminin receptor may show promise as possible prophylactic and/or therapeutic tools for the treatment of Alzheimer's disease.

Methods

Cell Culture. HEK293 cells were cultured in Dulbecco's Modified Eagle Medium (DMEM) (Hyclone) supplemented with 10% (v/v) Fetal Calf Serum (FCS) and 1% Penicillin/Streptomycin (P/S) solution and maintained in a humidified incubator (5% CO_2, 37°C).

Transient Transfection. Upon reaching 70% confluency HEK293 cells were transfected, by calcium phosphate methodology, with pCIneo-moLRP::FLAG (Vana and Weiss, 2006) or pCDNA/3CAT (Invitrogen) plasmids and were lysed 72 h post-transfection.

Pull down Assay. Samples were composed of 200 µl of LRP::FLAG containing whole cell lysates and 200 µl of either conditioned tissue culture media (containing shed Aβ) or lysates expressing Chloramphenicol Acetyl Transferase (CAT). Conditioned tissue culture media was similarly co-incubated with non-transfected (NT) whole cell lysates (lacking LRP::FLAG) as well as subjected alone to immunoprecipitation to account for non-specific binding to the anti-FLAG® M2 beads. FLAG® Immunopercipitation Kit (Sigma-Aldrich) assays were performed as per manufacturer's instructions. Samples were subsequently subjected to both electrophoretic and western blot analysis as well as Amyloid beta Enzyme-linked Immunosorbent Assays (ELISA). Three independent experiments were performed, each in triplicate.

Immunoblotting. FLAG® Immunoprecipitation assay eluate samples were detected using murine anti-FLAG antibody (1 : 4000) (Sigma-Aldrich) or anti-Chloramphenicol Acetyl Transferase (rabbit IgG fraction) (1 : 6000) (Sigma-Aldrich). The secondary antibodies employed were goat anti-mouse HRP (1 : 10 000) (Sigma-Aldrich) and anti-rabbit-HRP (1 : 10000) (Sigma-Aldrich), respectively. The loading control, β-actin, was detected employing the rabbit anti-β-actin-HRP antibody (1 : 10000) (Sigma-Aldrich). Experiments were performed in triplicate, three times.

Amyloid beta Enzyme-linked Immunosorbent Assay (ELISA). Post FLAG® immunoprecipitation, the Aβ concentration in each fraction was assessed by Human Amyloid β (1-x) Assay kit (Immuno-Biological Laboratories Co.,Ltd) – a solid phase ELISA, performed as per manufacturer instructions. Three independent experiments were performed, each in triplicate.

Flow cytometric analysis of Försters Resonance Energy Transfer (FRET). To assess FRET between LRP/LR and CAT, HEK cells were transfected to express recombinant CAT as described above. For the rest of the samples non-transfected HEK293 cells were employed. Cells were incubated in serum-free media for 3–4 h prior to assessment. Cells were detached (5 Mm EDTA-PBS), harvested in serum free media, centrifuged at 1200 rpm (4°C, 10 min), washed thrice in ice-cold D-PBS and fixed with ice-cold 2% PFA (20 min, 4°C). These non-permeabilized cells were again washed (1x PBS) and blocked in 0.5%PBS-BSA for 10 min. The primary antibody solutions (20 µg/ml) (diluted in 0.05% PBS-BSA) employed were: human IgG1-iS18 (Affimed Therapeutics); murine anti-PrP^c (Sigma-Aldrich); rabbit anti-CAT (Sigma-Aldrich) and rabbit anti-β-amyloid (22–35) (Sigma-Aldrich). The secondary antibody solutions (20 µg/ml) (diluted in 0.05% PBS-BSA) employed were: goat-anti-human-PE (Abcam) IgG1-iS18, goat-anti-mouse-APC (Abcam) and goat-anti-rabbit-APC (Abcam). The following samples were prepared: 1) unstained cells, 2) cells stained with goat-anti-human PE only; 3) cells labelled with goat-anti-mouse-APC only; 4) cells labelled with goat-anti-rabbit-APC only; 5) cells labelled with IgG1-iS18-PE (LRP/LR detection); 6) cells labelled with anti-PrP^c-APC (PrP^c detection), 7) cells labelled with anti-CAT-APC (CAT detection); cells labelled with anti-$A\beta_{42}$-APC ($A\beta_{42}$ detection), 8) cells labelled with IgG1-iS18-PE & anti-PrP^c-

APC; 9) cells labelled with IgG1-iS18-PE & anti-CAT-APC and 10) cells labelled with IgG1-iS18-PE & anti-$A\beta_{42}$-APC. Cells were incubated in primary antibody solutions for 2 h, washed twice in 1xPBS and once in 0.5% PBS-BSA and incubated in secondary antibody solutions for 2 h. The cells were washed thrice prior to analysis. Three biological replicates, each performed in triplicate, were conducted. In each sample, 10 000 cells were analysed.

Antibody Treatment. Varying concentrations (200 nM & 500 nM) synthetic Amyloid beta peptide 42 ($A\beta_{42}$) (Sigma-Aldrich) was administered to cells in the presence or absence of 50 μg/ml IgG1-iS18 (anti-LRP/LR specific antibody) (Affimed Therapeutics) or 50 μg/ml anti-Chloramphenicol Acetyl Transferase (CAT) (rabbit IgG fraction) (Sigma-Aldrich).

Annexin-V-7Aminoactinomycin D Assay. HEK293 cells were subjected to $A\beta_{42}$ and antibody treatment as detailed above. The degree of cell death attributable to apoptosis was assessed at 24 h, 48 h and 72 h post treatment using Annexin-V-FITC/7-AAD kit (Beckman Coulter) as per the manufacturer's instructions. The effects of antibody treatment on cell death was assessed after 72 h. Three biological replicates, each performed in triplicate, were conducted. In each sample, 10 000 cells were analysed.

Nuclear staining- Assessing Nuclear Morphology. HEK293 cells were seeded onto coverslips and were subjected to 500 nM $A\beta_{42}$ or 8 mM PCA (apoptosis inducing agent served as the positive control) treatment for 72 h. Cells were subsequently fixed (4% PFA, 15 min, 4°C), rinsed thrice (1xPBS) and blocked (0.5%PBS-BSA,10 min). Hoechst 33342 (1 : 100 dilution of 2 mg/ml stock solution) (Sigma-Aldrich) was administered for 5 min (RT) to cells which were subsequently rinsed and mounted onto microscope slides using 50 μl of Fluoromount (Sigma-Aldrich). Images were acquired using Zeiss LSM780 confocal microscope and Zen 2010 imaging software.

shRNA mediated downregulation of LRP. The TransIT®–LT1 Transfection reagent (Mirus) was employed, as per manufacturer's instructions, to transfect HEK293 cells with shRNA 1.1, shRNA 7.6 and shRNA scr (scrambled shRNA, negative control). The production of the shRNA targeting LRP/LR mRNA has been described previously[26,29].

Flow cytometric analysis of cell surface levels of LRP and PrP^c. Post LRP downregulation by shRNA methodology (72 h post transfection) cell surface LRP and PrP^c levels were assessed by flow cytometry. Cells were fixed in 4% paraformaldehyde (15 min, 4°C), washed thrice (1xPBS) and blocked (0.5%PBS-BSA, 10 min). Samples were halved, one half was subjected to both primary and secondary antibody treatments whilst only secondary antibody was administered to the other sample. Cells were incubated with primary antibodies (20 μg/ml), namely human IgG1-iS18 (anti-LRP/LR specific antibody) (Affimed therapeutics) and murine anti-PrP^c 8H4 (Sigma-Aldrich) for 3 h at RT, washed thrice and were treated with 10 μg/ml goat anti-human PE (Abcam) and goat anti-mouse APC (Abcam) secondary antibodies for 2 h. The cells washed thrice prior to analysis. Three biological replicates, each performed in triplicate, were conducted. In each sample, 10 000 cells were analysed.

Internalization Assay. Flow cytometric analysis was employed to assess the degree of $A\beta_{42}$ on the cell surface during different intervals during internalization. Cells (50% confluency) were either subjected to antibody treatments (50 μg/ml of IgG1-iS18 or anti-CAT) for 48 h or transfected with shRNAs and assessed 72 h post transfection. Cellular confluency of 70% was deemed optimal for internalization analysis. Cells were incubated in serum-free media for 3–4 h prior to assessment and subsequently subjected to 500 nM $A\beta_{42}$ treatment for 5 min, 15 min, 30 min and 1 h at 37°C in a 5% CO_2 humidified environment to allow for internalization. Cells were concomitantly incubated on ice at 4°C, for 30 min, after which 500 nM $A\beta_{42}$ was administered to cells and incubated at 4°C for 1 h. Incubation at 4°C arrests cell receptor mediated internalization (Li et al., 2008). Post treatment, cells were washed thrice(ice-cold 1xPBS), detached (5 Mm EDTA-PBS), harvested (ice-cold serum free media,1200 rpm,4°C, 10 min), washed again and fixed (ice-cold 4% PFA,20 min, 4°C). These non-permeabilized cells were again washed (1x PBS) and blocked (0.5%PBS-BSA, 10 min). Samples were halved, one half subjected to both antibody treatments whilst only secondary antibody was administered to the other sample. 100 μl of primary antibody solution containing 1 : 100 anti-β-amyloid (22–35) (rabbit) (Sigma-Aldrich) was administered to the cells and incubated for 2 h. Cells were washed and were treated with 10 μg/ml goat anti-rabbit APC (Abcam) secondary antibody for 2 h. Cells washed thrice prior to analysis. Three biological replicates, each performed in triplicate, were conducted. In each sample, 10 000 cells were analysed.

Immunofluorescence Microscopy. Cells (70% confluent) were transfected with pECFP-mem (Clonetech), a plasmid encoding N-terminal 20 amino acid fragment of neuromodulin which is fused to cyan-fluorescent protein (CFP)) thereby allowing for plasma membrane visualization. Post transfection, 48 h, cells were incubated in serum-free media for 3–4 h and subsequently subjected to 500 nM $A\beta_{42}$ for 5 min, 15 min and 30 min (37°C, 5%CO_2 humidified) to allow for internalization. Post treatment, the cells were placed on ice, washed thrice (ice-cold 1xPBS), fixed (4% PFA, 20 min, 4°C), rinsed thrice (ice-cold 1xPBS) and blocked (ice-cold 0.5%PBS-BSA containing 0.25% Triton X-100,10 min). Coverslips were again washed and incubated with the primary antibody solution - 1 : 100 anti-β-amyloid (22–35) (rabbit) (Sigma-Aldrich). Post overnight incubation (4°C) coverslips were again washed thrice in 0.5% PBS-BSA and incubated with the secondary antibody- 1 : 300 goat anti-rabbit APC (Abcam) for 1 h. Coverslips were washed twice in 0.5% PBS-BSA and once in 1xPBS and mounted onto clean microscope slides using 50 μl Fluoromount (Sigma-Aldrich). Images were acquired using Zeiss LSM780 confocal microscope and Zen 2010 imaging software.

Statistical Evaluation: Student's *t*-tests and ANOVAs were used to analyse the data and obtain p values. All statistical evaluations were performed using GraphPad Prism (version 5.03) software.

1. Suh, Y. H. & Checler, F. Amyloid precursor protein, presenilins, and alpha-synuclein: molecular pathogenesis and pharmacological applications in Alzheimer's disease. *Pharmacol. Rev.* **54**, 469–525 (2002).
2. Carter, M. D., Simms, G. A. & Weaver, D. F. The development of new therapeutics for Alzheimer's disease. *Clin. Pharmacol. Ther.* **88**, 475–486, DOI:10.1038/clpt.2010.165 (2010).
3. Behl, C., Davis, J. B., Lesley, R. & Schubert, D. Hydrogen peroxide mediates amyloid beta protein toxicity. *Cell* **77**, 817–827, DOI:0092-8674(94)90131-7 (1994).
4. Doecke, J. D. *et al.* Blood-based protein biomarkers for diagnosis of Alzheimer disease. *Arch. Neurol.* **69**, 1318–1325, DOI:10.1001/archneurol.2012.1282 (2012).
5. Haass, C., Kaether, C., Thinakaran, G. & Sisodia, S. Trafficking and proteolytic processing of APP. *Cold Spring Harb Perspect Med* **2**, a006270, DOI:10.1101/cshperspect.a006270 (2012).
6. Sandwall, E. *et al.* Heparan sulfate mediates amyloid-beta internalization and cytotoxicity. *Glycobiology* **20**, 533–541, DOI:10.1093/glycob/cwp205 (2010).
7. DeMattos, R. B. *et al.* Peripheral anti-A beta antibody alters CNS and plasma A beta clearance and decreases brain A beta burden in a mouse model of Alzheimer's disease. *Proc Natl Acad Sci U S A* **98**, 8850–8855, DOI:10.1073/pnas.151261398 (2001).
8. Parkin, E. T. *et al.* Cellular prion protein regulates beta-secretase cleavage of the Alzheimer's amyloid precursor protein. *Proc Natl Acad Sci U S A* **104**, 11062–11067, doi:0609621104 (2007).
9. Lauren, J., Gimbel, D. A., Nygaard, H. B., Gilbert, J. W. & Strittmatter, S. M. Cellular prion protein mediates impairment of synaptic plasticity by amyloid-beta oligomers. *Nature* **457**, 1128–1132, DOI:10.1038/nature07761 (2009).
10. Chen, S., Yadav, S. P. & Surewicz, W. K. Interaction between human prion protein and amyloid-beta (Abeta) oligomers: role OF N-terminal residues. *J Biol Chem* **285**, 26377–26383, DOI:M110.145516 (2010).
11. Mouillet-Richard, S. *et al.* Signal transduction through prion protein. *Science* **289**, 1925–1928 (2000).
12. Um, J. W. & Strittmatter, S. M. Amyloid-beta induced signaling by cellular prion protein and Fyn kinase in Alzheimer disease. *Prion* **7**, 37–41, DOI:10.4161/pri.22212 (2013).
13. Rushworth, J. V., Griffiths, H. H., Watt, N. T. & Hooper, N. M. Prion protein-mediated toxicity of amyloid-beta oligomers requires lipid rafts and the transmembrane LRP1. *J Biol Chem* **288**, 8935–8951, DOI:M112.400358 (2013).
14. Stahl, N., Borchelt, D. R., Hsiao, K. & Prusiner, S. B. Scrapie prion protein contains a phosphatidylinositol glycolipid. *Cell* **51**, 229–240 (1987).
15. Gauczynski, S. *et al.* The 37-kDa/67-kDa laminin receptor acts as the cell-surface receptor for the cellular prion protein. *EMBO J* **20**, 5863–5875, DOI:10.1093/emboj/20.21.5863 (2001).
16. Venticinque, L., Jamieson, K. V. & Meruelo, D. Interactions between laminin receptor and the cytoskeleton during translation and cell motility. *PLoS One* **6**, e15895, DOI:10.1371/journal.pone.0015895 (2011).
17. Mbazima, V., Da Costa Dias, B., Omar, A., Jovanovic, K. & Weiss, S. F. Interactions between PrP(c) and other ligands with the 37-kDa/67-kDa laminin receptor. *Front Biosci* **15**, 1150–1163, DOI:3667 (2010).
18. Omar, A. *et al.* Patented biological approaches for the therapeutic modulation of the 37 kDa/67 kDa laminin receptor. *Expert Opin Ther Pat* **21**, 35–53, DOI:10.1517/13543776.2011.539203 (2011).
19. Khumalo, T. *et al.* Adhesion and Invasion of Breast and Oesophageal Cancer Cells Are Impeded by Anti-LRP/LR-Specific Antibody IgG1-iS18. *PLoS One* **8**, e66297, DOI:10.1371/journal.pone.0066297 (2013).
20. Khusal, R. *et al.* In vitro inhibition of angiogenesis by antibodies directed against the 37 kDa/67 kDa laminin receptor. *PLoS One* **8**, e58888, DOI:10.1371/journal.pone.0058888 PONE-D-12-36507 (2013).
21. Wang, K. S., Kuhn, R. J., Strauss, E. G., Ou, S. & Strauss, J. H. High-affinity laminin receptor is a receptor for Sindbis virus in mammalian cells. *J. Virol.* **66**, 4992–5001 (1992).
22. Thepparit, C. & Smith, D. R. Serotype-specific entry of dengue virus into liver cells: identification of the 37-kilodalton/67-kilodalton high-affinity laminin receptor as a dengue virus serotype 1 receptor. *J. Virol.* **78**, 12647–12656, DOI:78/22/12647 (2004).
23. Akache, B. *et al.* The 37/67-kilodalton laminin receptor is a receptor for adeno-associated virus serotypes 8, 2, 3, and 9. *J. Virol.* **80**, 9831–9836, DOI:10.1128/JVI.00878-06 (2006).
24. Ludwig, G. V., Kondig, J. P. & Smith, J. F. A putative receptor for Venezuelan equine encephalitis virus from mosquito cells. *J. Virol* **70**, 5592–5599 (1996).

25. Orihuela, C. J. *et al*. Laminin receptor initiates bacterial contact with the blood brain barrier in experimental meningitis models. *J. Clin.Invest.* **119**, 1638–1646, DOI:10.1172/JCI36759 (2009).
26. Dias Bda, C. *et al*. Anti-LRP/LR specific antibody IgG1-iS18 and knock-down of LRP/LR by shRNAs rescue cells from Abeta42 induced cytotoxicity. *Sci Rep* **3**, 2702, DOI:srep02702 (2013).
27. Glazer, A. N. & Stryer, L. Fluorescent tandem phycobiliprotein conjugates. Emission wavelength shifting by energy transfer. *Biophys J* **43**, 383–386, DOI:10.1016/S0006-3495(83)84361-6 (1983).
28. Batard, P. *et al*. Use of phycoerythrin and allophycocyanin for fluorescence resonance energy transfer analyzed by flow cytometry: advantages and limitations. *Cytometry* **48**, 97–105, DOI:10.1002/cyto.10106 (2002).
29. Jovanovic, K. *et al*. Anti-LRP/LR specific antibodies and shRNAs impede amyloid beta shedding in Alzheimer's disease. *Sci Rep* **3**, 2699, DOI:srep02699 (2013).
30. Li, N., Hill, K. S. & Elferink, L. A. Analysis of receptor tyrosine kinase internalization using flow cytometry. *Methods Mol Biol* **457**, 305–317 (2008).
31. Da Costa Dias, B., Jovanovic, K., Gonsalves, D. & Weiss, S. F. Structural and mechanistic commonalities of amyloid-beta and the prion protein. *Prion* **5**, 126–137, DOI:10.4161/pri.5.3.17025 (2011).
32. Selvin, P. R. The renaissance of fluorescence resonance energy transfer. *Nature Struct. Biol.* **7**, 730–734, DOI:10.1038/78948 (2000).
33. Kumar, A., Kremer, K. N., Sims, O. L. & Hedin, K. E. Measuring the proximity of T-lymphocyte CXCR4 and TCR by fluorescence resonance energy transfer (FRET). *Methods Enzymol.* ***460***, 379–397, DOI:10.1016/S0076-6879(09)05219-7 (2009).
34. Behl, C., Davis, J. B., Klier, F. G. & Schubert, D. Amyloid beta peptide induces necrosis rather than apoptosis. *Brain Res* **645**, 253–264 (1994).
35. Sepulveda, F. J., Parodi, J., Peoples, R. W., Opazo, C. & Aguayo, L. G. Synaptotoxicity of Alzheimer beta amyloid can be explained by its membrane perforating property. *PLoS One* **5**, e11820, DOI:10.1371/journal.pone.0011820 (2010).
36. Givant-Horwitz, V., Davidson, B. & Reich, R. Laminin-induced signaling in tumor cells: the role of the M(r) 67,000 laminin receptor. *Cancer Res.* **64**, 3572–3579, DOI:10.1158/0008-5472.CAN-03-3424 (2004).
37. Selleri, C. *et al*. The metastasis-associated 67-kDa laminin receptor is involved in G-CSF-induced hematopoietic stem cell mobilization. *Blood* **108**, 2476–2484, DOI:10.1182/blood-2005-11-012625 (2006).
38. Zhao, W. Q. *et al*. MAP kinase signaling cascade dysfunction specific to Alzheimer's disease in fibroblasts. *Neurobiol. Dis.* **11**, 166–183 (2002).
39. Tsukamoto, S. *et al*. Green tea polyphenol EGCG induces lipid-raft clustering and apoptotic cell death by activating protein kinase Cdelta and acid sphingomyelinase through a 67 kDa laminin receptor in multiple myeloma cells. *Biochem. J* **443**, 525–534, DOI:10.1042/BJ20111837 (2012).
40. Ferreiro, E., Oliveira, C. R. & Pereira, C. M. The release of calcium from the endoplasmic reticulum induced by amyloid-beta and prion peptides activates the mitochondrial apoptotic pathway. *Neurobiol. Dis.* **30**, 331–342, DOI:10.1016/j.nbd.2008.02.003 (2008).
41. Hyeon, J. W. *et al*. The association between prion proteins and Abeta(1)(-)(4)(2) oligomers in cytotoxicity and apoptosis. *Biochem. Biophys. Res. Commun.* **424**, 214–220, DOI:10.1016/j.bbrc.2012.06.056 (2012).
42. Neniskyte, U., Neher, J. J. & Brown, G. C. Neuronal death induced by nanomolar amyloid beta is mediated by primary phagocytosis of neurons by microglia. *J Biol Chem* **286**, 39904–39913, DOI:10.1074/jbc.M111.267583 (2011).
43. Sengupta, P. *et al*. The amyloid beta peptide (Abeta(1-40)) is thermodynamically soluble at physiological concentrations. *Biochemistry* **42**, 10506–10513, DOI:10.1021/bi0341410 (2003).
44. Hu, X. *et al*. Amyloid seeds formed by cellular uptake, concentration, and aggregation of the amyloid-beta peptide. *Proc Natl Acad Sci U S A* **106**, 20324–20329, DOI:10.1073/pnas.0911281106 (2009).
45. Gong, Y. *et al*. Alzheimer's disease-affected brain: presence of oligomeric A beta ligands (ADDLs) suggests a molecular basis for reversible memory loss. *Proc Natl Acad Sci U S A* **100**, 10417–10422, DOI:10.1073/pnas.1834302100 (2003).
46. Leucht, C. *et al*. The 37 kDa/67 kDa laminin receptor is required for PrP(Sc) propagation in scrapie-infected neuronal cells. *EMBO Rep.* **4**, 290–295, DOI:10.1038/sj.embor.embor768 (2003).
47. Morel, E. *et al*. Bovine prion is endocytosed by human enterocytes via the 37 kDa/67 kDa laminin receptor. *Am J Pathol* **167**, 1033–1042, DOI:S0002-9440(10)61192-3 (2005).
48. Cisse, M. & Mucke, L. Alzheimer's disease: A prion protein connection. *Nature* **457**, 1090–1091, DOI:10.1038/4571090a (2009).
49. Sakono, M. & Zako, T. Amyloid oligomers: formation and toxicity of Abeta oligomers. *FEBS J.* **277**, 1348–1358, DOI:10.1111/j.1742-4658.2010.07568 (2010).
50. Um, J. W. *et al*. Metabotropic glutamate receptor 5 is a coreceptor for Alzheimer abeta oligomer bound to cellular prion protein. *Neuron* **79**, 887–902, DOI:S0896-6273(13)00552-7 (2013).
51. Leucht, C. *et al*. Knock-down of the 37-kDa/67-kDa laminin receptor in mouse brain by transgenic expression of specific antisense LRP RNA. *Transgenic. Res.* **13**, 81–85 (2004).

Acknowledgments

This work is based upon research supported by the National Research Foundation (NRF), the Republic of South Africa (RSA). Any opinions, findings and conclusions or recommendations expressed in this material are those of the author(s), and therefore, the National Research Foundation does not accept any liability in this regard thereto.

Author contributions

Conceived and designed the experiments: B.D.C.D., S.F.T.W. Design of shRNA: M.S.W. Production of shRNA: D.G., K.M. Performed experiments: B.D.C.D. Antibody (IgG1-iS18) production: U.R., S.K. and M.L. Analysed data: B.D.C.D. Wrote the manuscript: B.D.C.D. Edited the manuscript: B.D.C.D., K.J. and S.F.T.W.

Additional information

Supplementary information accompanies this paper at http://www.nature.com/scientificreports

Competing financial interests: The authors declare no competing financial interests.

How to cite this article: Da Costa Dias, B. *et al*. The 37kDa/67kDa Laminin Receptor acts as a receptor for $A\beta_{42}$ internalization. *Sci. Rep.* **4**, 5556; DOI:10.1038/srep05556 (2014).